Generation of mouse conditional knockout alleles in one step using the *i*-GONAD method

Renjie Shang,[1,2] Haifeng Zhang,[1] and Pengpeng Bi[1,2]

[1] *Center for Molecular Medicine, University of Georgia, Athens, Georgia 30602, USA;* [2] *Department of Genetics, University of Georgia, Athens, Georgia 30602, USA*

The Cre/*loxP* system is a powerful tool for gene function study in vivo. Regulated expression of Cre recombinase mediates precise deletion of genetic elements in a spatially– and temporally–controlled manner. Despite the robustness of this system, it requires a great amount of effort to create a conditional knockout model for each individual gene of interest where two *loxP* sites must be simultaneously inserted in *cis*. The current undertaking involves labor-intensive embryonic stem (ES) cell–based gene targeting and tedious micromanipulations of mouse embryos. The complexity of this workflow poses formidable technical challenges, thus limiting wider applications of conditional genetics. Here, we report an alternative approach to generate mouse *loxP* alleles by integrating a unique design of CRISPR donor with the new oviduct electroporation technique *i*-GONAD. Showing the potential and simplicity of this method, we created floxed alleles for five genes in one attempt with relatively low costs and a minimal equipment setup. In addition to the conditional alleles, constitutive knockout alleles were also obtained as byproducts of these experiments. Therefore, the wider applications of *i*-GONAD may promote gene function studies using novel murine models.

[Supplemental material is available for this article.]

Our understanding of the genetic mechanisms of human diseases has been largely expanded by loss-of-function studies using engineered mouse models. Two types of gene knockout mouse models are commonly used: global and conditional, each with unique advantages. Ubiquitous deletion of a gene from all tissues in a global knockout model can mimic the genetic condition of human disease, thus permitting a quick and thorough evaluation of gene function in vivo (Cheon and Orsulic 2011; Doyle et al. 2012; Wang et al. 2013; Amoasii et al. 2017; Gurumurthy and Lloyd 2019). Given the flexible design of gene inactivation, for example, frame shift mutation caused by a small insertion or deletion (indel) or targeted removal of exon(s), the design and creation of a global knockout mouse model is relatively easy. However, genetic studies using this type of model may have inherent limitations. First, for a gene that is widely expressed, pleiotropic effects from its deletion in all tissues can obscure the cell type–specific gene functions. Second, an early onset lethality or gross abnormality of a mutant will prevent its application for studying gene function at adult stages or during aging conditions.

Cre/*loxP*-mediated conditional knockout models can circumvent these difficulties. Cre can delete the flanked gene sequence between two *loxP* sites through DNA recombination (Sauer and Henderson 1988). Built on this principle, more sophisticated models of hormone-sensitive or tetracycline-inducible conditional knockouts were developed that allowed precise temporal control of gene disruption (Danielian et al. 1998; Jaisser 2000; Schonig et al. 2002; Belteki et al. 2005; Feil et al. 2009). These models have afforded valuable opportunities to interrogate the context-dependent gene function, thus providing clinically relevant information to treat genetic disease. The Cre/*loxP* system requires the creation of a conditional allele for the gene of interest. Although many tissue-specific/hormone-inducible Cre-expressing mouse strains are readily available, generation of the *loxP*-flanked (floxed) alleles is challenging and labor-intensive due to the lack of an efficient method for their generation (Lewandoski 2001; Skarnes et al. 2011; Bouabe and Okkenhaug 2013).

The common approach for generating floxed alleles was established in the 1980s (Thomas and Capecchi 1987; Mansour et al. 1988; Capecchi 1989; Zijlstra et al. 1989; te Riele et al. 1992; Limonta et al. 1995; Skarnes 2015). It utilizes homologous recombination in embryonic stem cells and requires technically challenging embryo-manipulation procedures. Such practice is largely restricted to transgenic core facilities, making the approach costly, time-consuming, and lacking in guaranteed success. Although this method has cumulatively created many invaluable mouse models over the past decades (Skarnes et al. 2011), scaling this approach up to functionally characterize the vast majority of the genome, with its rapidly expanding gene list (Chen et al. 2020) and associated genetic elements, is a challenging endeavor. Therefore, an alternative method that is inexpensive and easy to implement is awaited by the mouse genetic research community. Ideally, such methodology can be performed by regular laboratory personnel, for example, graduate students, with necessary technical training. Toward this goal, both the gene targeting strategy and the delivery method should be streamlined.

CRISPR genome-editing technologies have revolutionized genetic studies (Hsu et al. 2014; Irion et al. 2014; Platt et al. 2014; Aida et al. 2015; Square et al. 2015; Wang et al. 2016a; Zu et al. 2016; Jiang and Doudna 2017; Adli 2018; Miura et al. 2018; Gurumurthy and Lloyd 2019; Rasys et al. 2019; Yuan et al. 2019). However, successful applications of CRISPR-based mutagenesis have been largely restricted to creation of global loss-of-

Corresponding author: pbi@uga.edu
Article published online before print. Article, supplemental material, and publication date are at http://www.genome.org/cgi/doi/10.1101/gr.265439.120.

function models. Compared with random indels, the efficiency of precise editing through homology-mediated repair (HDR) is low (Doudna and Charpentier 2014; Jiang and Marraffini 2015; Richardson et al. 2016; Zhang et al. 2017; Aird et al. 2018). Because the generation of conditional alleles requires simultaneous integration of two *loxP* sites precisely in the same chromosomal region (in *cis*), the chance of success is significantly lower when compared with other HDR projects.

Single-stranded oligo DNA (ssODNA) that contains homologous sequences flanking the nuclease-induced dsDNA break site emerged as an ideal form of HDR template that delivers higher knock-in efficiency and specificity (Miura et al. 2015; Yoshimi et al. 2016). A recent study of the interactions between the Cas9 protein with its DNA substrate provided a rational to improve the HDR design (Richardson et al. 2016). Specifically, asymmetric target-strand ssODNAs were shown to be highly effective in introducing point mutations (Richardson et al. 2016). Using this type of ssODNA, we previously generated two conditional alleles for the *Mymx* gene by microinjection with an overall 12% efficiency (Bi et al. 2018). It should be noted, however, that an independent test of *loxP* insertions for 30 genes showed a nonsignificant impact of homology arm symmetry on HDR efficiency (Lanza et al. 2018). Reported in this large-scale test, the efficiency of *loxP* insertion by using short ssODNA, either symmetric or asymmetric designs, is around 9% (Lanza et al. 2018). More recently, utilizing various types of short ssODNA to separately insert *loxP* sites, extensive efforts from a consortium of core facilities and laboratories reported an overall 1% efficiency on 56 loci (Gurumurthy et al. 2019a). These studies revealed large disparities of the gene targeting efficiency through microinjection.

In addition to microinjection, alternative CRISPR delivery methods were reported (Kaneko and Mashimo 2015; Takahashi et al. 2015; Gurumurthy et al. 2016; Wang et al. 2016b; Modzelewski et al. 2018; Ohtsuka et al. 2018; Teixeira et al. 2018). Of special interest, a mouse zygote-stage embryo transfection strategy called improved-Genome editing via Oviductal Nucleic Acids Delivery (*i*-GONAD) was reported (Ohtsuka et al. 2018). This method delivers a gene editing cocktail into mouse zygotes through oviduct electroporation. Operation of *i*-GONAD is easier than the ES-cell-based approach or microinjection because mouse zygotes no longer need to be individually handled and transferred into pseudopregnant mice (Ohtsuka et al. 2018; Gurumurthy et al. 2019b), yet the HDR efficiency of *i*-GONAD was comparable to that achieved through microinjection (Ohtsuka et al. 2018). For the creation of conditional alleles, one recent study proposed a two-step *i*-GONAD workflow that sequentially inserts two *loxP* sites, one at a time (Sato et al. 2020). However, the proof-of-principle test of this approach was not satisfactory, that is, only one *loxP* was integrated (Sato et al. 2020). Therefore, both the CRISPR targeting strategy and the logistics of *i*-GONAD for creation of conditional alleles require improvement. Here, we aim to develop and test a new approach by integrating a unique design of asymmetric *loxP*-ssODNA with the *i*-GONAD delivery method to create mouse conditional alleles.

Results

Exploiting the *i*-GONAD method to create a conditional allele: a proof-of-principle test

The principle of HDR template design, major experimental procedures, and milestones for this method are schematized in Figure 1A.

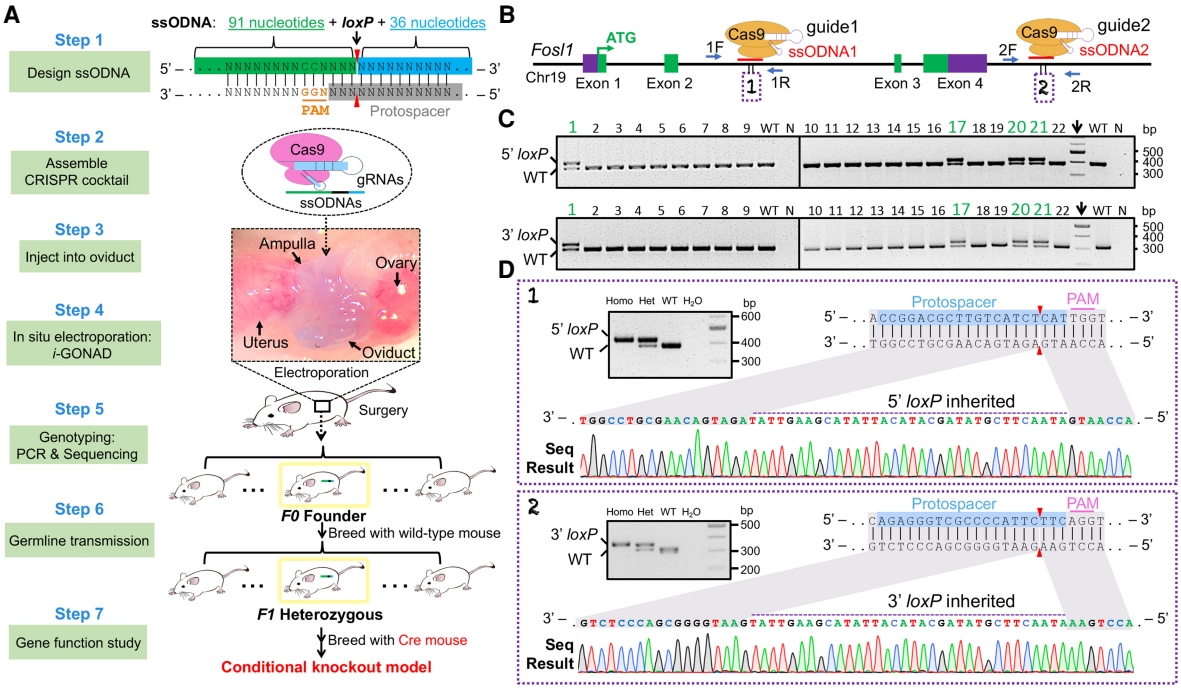

Figure 1. Generation of a conditional allele by *i*-GONAD: design and a proof-of-principle test. (*A*) Schematic illustration of the strategy to generate a conditional allele by *i*-GONAD. The necropsy image was taken to show the anatomical location of the oviduct with a blue ink indicator. (*B*) *Fosl1* gene structure and relative positions of ssODNA, gRNA, and genotyping primer. (ssODNA) Single-stranded oligo DNA. (*C*) *Fosl1* genotyping results for the *F1* generation. *Top* row detects 5′-*loxP* insertion by primer pair 1F&1R; *bottom* row detects 3′-*loxP* insertion by primer pair 2F&2R; 5′-*loxP* band size is 426 bp; 3′-*loxP* is 351 bp. Mouse that inherited both 5′- and 3′-*loxP* is highlighted in green. (Arrow) DNA marker lane, (N) negative control of PCR (water). (*D*) Validations of *loxP* sites by Sanger sequencing.

It involves using two guide RNAs (gRNAs) and two short ssODNAs as HDR donors for *loxP* insertions. Each ssODNA is 161 nt long, composed of 91 nt of the 5′ homology arm from the PAM-proximal side, 34 nt of *loxP* sequence, and 36 nt of the 3′ homology arm from the PAM-distal side.

We first tested the *i*-GONAD method by generating a mouse conditional allele for the *Fosl1* (fos-like antigen 1) gene for which the expression at both mRNA and protein levels was induced during muscle regeneration (Supplemental Fig. S1). The function of the *Fosl1* gene during this biological process remains unknown. Because *Fosl1* global knockout mice die as embryos (Schreiber et al. 2000), studying the postnatal muscle-specific function of this gene requires a conditional allele.

The mouse *Fosl1* gene contains four exons, with the last two being close to each other and representing 64% of the coding sequence including critical domains of the FOSL1 protein (Matsuo et al. 2000). Therefore, deletions of exons 3 and 4 can unequivocally abolish gene function. We designed a pair of gRNAs and the corresponding ssODNAs to insert *loxP* sites flanking these exons (Fig. 1B). Different from microinjection, which directly delivers CRISPR components into the zygotes, *i*-GONAD involves a two-step transfer of the gene editing cocktail: first, the cocktail is injected into the lumen of the oviduct, followed by a second step of oviduct electroporation that transfers the cocktail into zygotes (Fig. 1A; Ohtsuka et al. 2018). Owing to the volume restriction of the oviduct and inevitable dilutions of the gene editing cocktail by the much larger volume of oviduct fluid, we used concentrated Cas9 protein, ssODNAs, and gRNAs in molar ratios of 1:6:10, as we previously used in microinjection experiments (Bi et al. 2018).

CD-1 female mice in estrus were mated with C57BL/6J males. We performed *i*-GONAD on two females that showed copulation plugs. To avoid false detection of *loxP* sites in scenarios of random ssODNA integration, genotyping primers were designed in the regions outside the homology arms of donors. Successful incorporation of *loxP* was identified by a 34-base-pair (bp) increase in PCR amplicon size. Our results revealed the simultaneous 5′- and 3′-*loxP* insertions in one mouse (#2) (Supplemental Fig. S2). We also detected 5′- or 3′-*loxP* integrations in other mice: #1, #10, #11, #14, #15, and #20 (Supplemental Fig. S2). Because transgenic founders are commonly mosaic, we tested germline editing of the #2 mouse by breeding it with wild-type (WT) mice. Out of a total of 22 filial 1 (*F1*) progenies obtained, four showed simultaneous inheritance of 5′- and 3′-*loxP* sites (Fig. 1C). The fidelity of these *loxP* sites was also validated by sequencing (Fig. 1D). Intercrossing of the heterozygous mice generated homozygous $Fosl1^{loxP/loxP}$ mutants at expected Mendelian ratios. These mutants appeared phenotypically normal, indicating that *loxP* insertions do not alter gene function, a prerequisite for conditional alleles.

More tests of the *i*-GONAD method to create conditional alleles for another four genes

To our knowledge, the $Fosl1^{loxP}$ allele is the first conditional allele created by the *i*-GONAD protocol in one step, which is easier and faster than two-step approaches. To better evaluate the efficiency, we performed additional tests on four other genes: *Plagl1* (pleiomorphic adenoma gene-like 1), *Ak040954*, *Clcf1* (cardiotrophin-like cytokine factor 1), and *Gm44386*. In addition to having different genomic locations, these genes were chosen because of our research interests, their distinct functions, and patterns of epigenetic regulations (Fig. 2A). As such, tests on these loci may demonstrate the broader utility of this method.

We first tested the synergy and editing efficiency of gRNAs in mouse fibroblasts (Supplemental Fig. S3). The gRNA pair that can generate large deletions between the gRNAs was chosen for *i*-GONAD. The *loxP* sequence contains an 8-bp asymmetric core spacer that defines the orientation of the *loxP* cassette (Sternberg et al. 1981; Sauer and Henderson 1988). Deletion of the flanked sequence requires that the two *loxP* sites are aligned in the same direction (Guo et al. 1997). We therefore adjusted the orientation of the *loxP* sequence within the HDR donors when gRNAs targeted opposite DNA strands.

For the *Plagl1* gene, we aimed to generate a conditional allele by flanking the coding exons 5 and 6 with *loxP* sites (Fig. 2B). Four females were used for the *i*-GONAD procedure. Among 28 pups that were born, three (#8, #10, #11) showed simultaneous 5′- and 3′-*loxP* insertions, and another eight mice showed either 5′- or 3′-*loxP* insertions (Supplemental Fig. S4A). Among 15 progeny obtained from breeding the #10 founder with C57BL/6J WT mice, eight pups showed successful germline transmission of both *loxP* sites (Supplemental Fig. S4B). Correct targeting in these mice was also confirmed by sequencing (Fig. 2B, boxed panels). Of note, all other progeny showed the insertion of only the 3′-*loxP* site (Supplemental Fig. S4B). This reveals the mosaicism of genome editing.

The long noncoding gene *Ak040954* contains two exons. We targeted the major exon 2 which represents 91% of the transcript (Fig. 2C). Three female mice were used for *i*-GONAD. Among 11 mice that were born, two pups (#5, #7) showed simultaneous 5′- and 3′-*loxP* insertions, whereas another two pups (#8, #9) showed only 5′-*loxP* insertions (Supplemental Fig. S4C). Among nine progeny obtained from breeding of #5 founder with C57BL/6J WT, three pups showed successful germline transmissions of floxed alleles that contained both the 5′- and 3′-*loxP* sites (Supplemental Fig. S4D). The fidelity of *loxP* sequences was validated by sequencing (Fig. 2C, boxed panels). We also observed the inheritance of other types of mutations, showing up as >34 bp insertions (#2, #7) (Supplemental Fig. S4D), which mirrored the genotype of their *F0* parent (Supplemental Fig. S4C).

The *Clcf1* gene contains three exons that together encode a 225-amino acid cytokine. We generated a conditional knockout allele by targeting exon 3 (Fig. 2D) that encodes the majority of the protein. Among eight pups produced, one mouse (#2) showed simultaneous 5′- and 3′-*loxP* insertions, and another two mice (#1, #4) showed either 3′- or 5′-*loxP* insertion, respectively (Supplemental Fig. S4E). Among 13 progeny of the #2 founder, eight mice showed successful germline transmissions of both 5′- and 3′-*loxP* insertions (Supplemental Fig. S4F). The fidelity of *loxP* sites was also confirmed by sequencing (Fig. 2D, boxed panels). All other pups showed only 5′-*loxP* insertions (Supplemental Fig. S4F). This is consistent with the genotype of the *F0* founder for which the 5′-*loxP* insertion was nearly homozygous (Supplemental Fig. S4E).

Using the *i*-GONAD method, we also generated a conditional allele for the *Gm44386* gene, whereby the coding exons were flanked by two *loxP* sites (Fig. 2E). Among nine pups produced, two (#1, #5) showed simultaneous 5′- and 3′-*loxP* insertions, whereas another two (#3, #9) showed only 3′-*loxP* insertions (Supplemental Fig. S4G). Successful transmissions of the two *loxP* sites were also confirmed by PCR (Supplemental Fig. S4H) and sequencing (Fig. 2E, boxed panels).

A

Gene	Gene locus[1]	Molecular type[2]	Expression[3]	Imprinted
Plagl1	Chr10: 13,090,788–13,131,694	Transcription factor	Endocardial cell	Yes
Ak040954	Chr12: 32,751,319–32,770,956	Unknown	Unknown	N/A
Clcf1	Chr19: 4,214,238–4,223,490	Cytokine	Satellite cell	N/A
Gm44386	Chr6: 86,513,891–86,516,273	lncRNA	Unknown	N/A

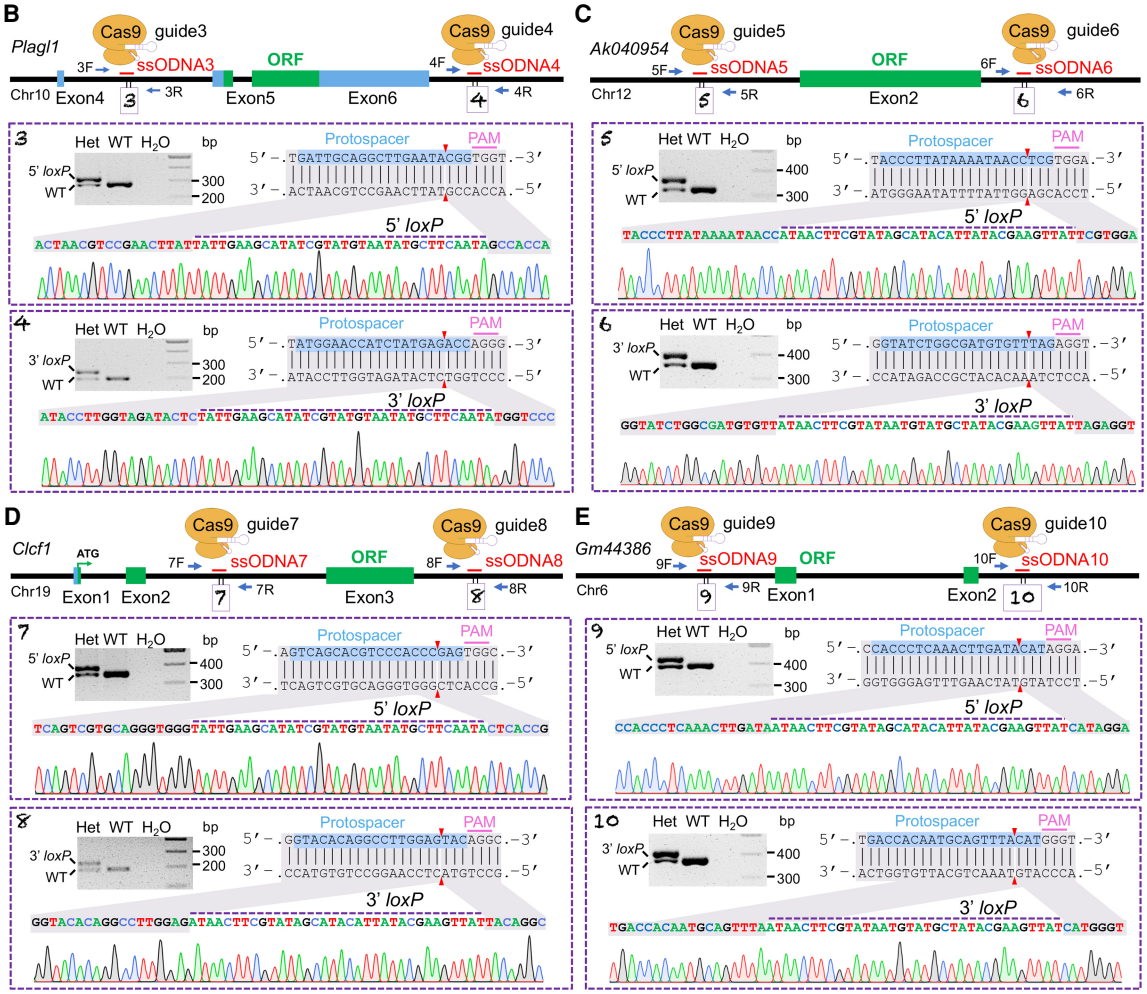

Figure 2. Generation of conditional alleles for another four genes by the *i*-GONAD method. (*A*) Gene information: [1]coordinates as of mouse GRCm38/mm10 genome assembly; [2]NCBI annotation; [3]query of *Tabula Muris* single-cell RNA sequencing data. (N/A) Data not available. (*B–E*) Gene structures and relative positions of ssODNA, gRNA, and genotyping primer for *Plagl1* (*B*), *Ak040954* (*C*), *Clcf1* (*D*), and *Gm44386* (*E*) genes. For *Plagl1*, 5′- and 3′-*loxP* bands are 312 bp and 234 bp; for *Ak040954*, 5′- and 3′-loxP bands are 361 bp and 391 bp; for *Clcf1*, 5′- and 3′-*loxP* bands are 389 bp and 222 bp; for *Gm44386*, 5′- and 3′-*loxP* bands are 431 bp and 415 bp. Boxed panels showed sequencing verifications of *loxP* sites in *F1* generations. (Het) Heterozygous.

A cloning-based strategy to rapidly identify founders with *loxP* insertions in *cis*

By Mendel's law of inheritance, the simultaneous transmission of 5′- and 3′-*loxP* sites into the *F1* generation validated *loxP* insertions in *cis* for five founders, that is, one for each gene. In addition to these mice, we also obtained other *F0* founders that showed both 5′- and 3′-*loxP* sites. This includes the #5 mouse for the *Gm44386* gene (Supplemental Fig. S4G), the #7 mouse for the *Ak040954* gene (Supplemental Fig. S4C), and the #8 and #11 mice for the *Plagl1* gene (Supplemental Fig. S4A). To deconvolute the potential mosaicism in these *F0* founders (Fig. 3A) and identify more floxed alleles, we devised a cloning-based strategy of genotyping.

As illustrated in Figure 3B, long-range genotyping PCR was performed with the forward primer from the 5′ gRNA region (5′F) and the reverse primer from 3′ gRNA region (3′R). Because the sizes of these PCR products were large (Fig. 3B), gel electrophoresis cannot reliably identify floxed alleles from others, for example, single *loxP*, WT, or small indels. We leveraged the principle of molecular cloning to genotype a single DNA molecule amplified by the long-range PCR (Fig. 3B). During transformation, the plasmid incompatibility ensures that each bacterium only maintains one

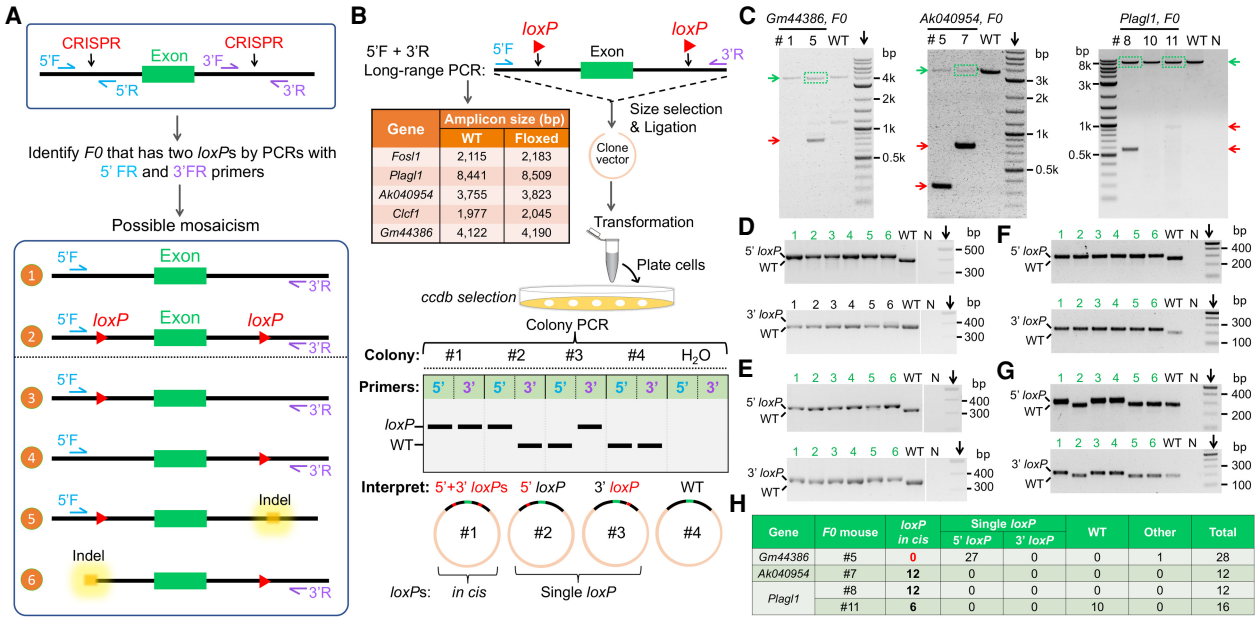

Figure 3. Validations of floxed alleles by long-range genotyping PCR. (*A*) Illustration of the potential mosaicism of *F0* founders. Although founders with 5′- and 3′-*loxP* insertions can be separately identified by genotyping PCR using 5′F + 5′R and 3′F + 3′R primers, this cannot distinguish whether *loxP* insertions are in *cis* or in *trans*. (*B*) Schematic to show the design and major steps of genotyping strategy. (*C*) DNA electrophoresis results of long-range PCR. The DNA bands enclosed in the green box were purified and cloned into vectors. (*D*–*G*) Representative genotyping results of bacterial colonies from cloning of the purified long-range PCR products for founder #5 of the *Gm44386* gene (*D*), founder #7 for the *Ak040954* gene (*E*), and founder #8 (*F*) and #11 (*G*) for the *Plagl1* gene. (*H*) Summary of bacterial colony genotyping results.

vector that hosts one DNA insert. This provides an opportunity to verify the presence of two *loxP* sites in a single DNA molecule through genotyping the bacterial colony using 5′F&5′R and 3′F&3′R primers, which give rise to much shorter amplicons that can be analyzed by regular gel electrophoresis (Fig. 3B). In rare cases where a competent cell takes more than one vector, such heterogeneity can also be detected by PCR and will be excluded from analyses.

As expected, the separation of long-range PCR products by electrophoresis is poor (green arrows, Fig. 3C). To reduce the cloning background, we purified the large amplicons (green boxes, Fig. 3C) for ligations. Genotyping results of bacterial colonies for the #5 mouse of the *Gm44386* gene showed only 5′ *loxP*, whereas the 3′ gRNA region was WT-size (Fig. 3D). Mimicking the bacterium genotyping results, the progeny of this mouse only showed 5′ *loxP* (Supplemental Fig. S4I). Compared with the genotype of this founder (Supplemental Fig. S4G), these observations indicate a mosaicism that possibly includes scenarios #3 and #6 illustrated in Figure 3A (lower panel). In comparison, floxed alleles were detected for all other founder mice (Fig. 3E–H). As a validation, breeding of the #7 mouse (*Ak040954*) produced *F1* progeny that contained both *loxP* sites (three out of 10 pups). Together, these experiments proved the accuracy of the cloning-based method to identify floxed alleles.

Byproducts of the *i*-GONAD method can serve as global knockout models

The long-range PCR revealed large-deletion alleles from these *i*-GONAD experiments (red arrows, Fig. 3C). Indeed, deletions of various sizes were observed for all five genes (Fig. 4A–D; Supplemental Figs. S5–S7). In total, 20 out of 54 (37%) *F0* generation mice showed large deletions. As a consequence, critical exons for these genes were removed as confirmed by sequencing. This includes deletions of 7489 bp for the *Plagl1* gene (Supplemental Fig. S5C), 3413 bp for the *Ak040954* gene (Fig. 4E), 3664 bp for the *Gm44386* gene (Fig. 4F), 1812 bp for the *Fosl1* gene (Supplemental Fig. S6B), and 1755 bp for the *Clcf1* gene (Supplemental Fig. S7B). Note that the amplicons for WT or floxed alleles were too large and thus not detected in these PCR conditions. Collectively, these "byproduct" mutants obtained from *loxP* projects may serve as global knockout models.

Other types of mutations from the *F0* generation included smaller indels produced by either 5′- or 3′-gRNA, for example, mice #15 and #20 for the *Fosl1* gene (Supplemental Fig. S2), and mice #1, #2, #6, and #8 for the *Clcf1* gene (Supplemental Fig. S4E). In scenarios where intron-exon splicing sites were destroyed, abnormal splicing may join incompatible exons, making these mutations potentially useful as knockout or hypomorphic alleles.

Examination of off-target mutagenesis by *i*-GONAD

The high efficiency of *i*-GONAD prompted us to examine the genome editing specificity in *F0* founders that contained floxed alleles (Supplemental Fig. S8A). We used the polyacrylamide gel electrophoresis (PAGE) method (Zhu et al. 2014) to quickly and sensitively detect small indels. Among 10 gRNAs, #2 gRNA produced off-target mutagenesis in the predicted site (Supplemental Fig. S8A–C). Coincidently, only this off-target site had identical sequence with the 10-bp PAM-proximal "seed" region of the gRNA (Supplemental Fig. S8A). This aligns with the notion that a single nucleotide mismatch within the PAM-proximal region is not tolerated by the CRISPR-Cas9 (Qi et al. 2013; Fortin et al. 2019). Together, our results showed that genome editing delivered by *i*-GONAD is largely specific, though caution is also warranted when gRNAs with predicted low-specificity were used.

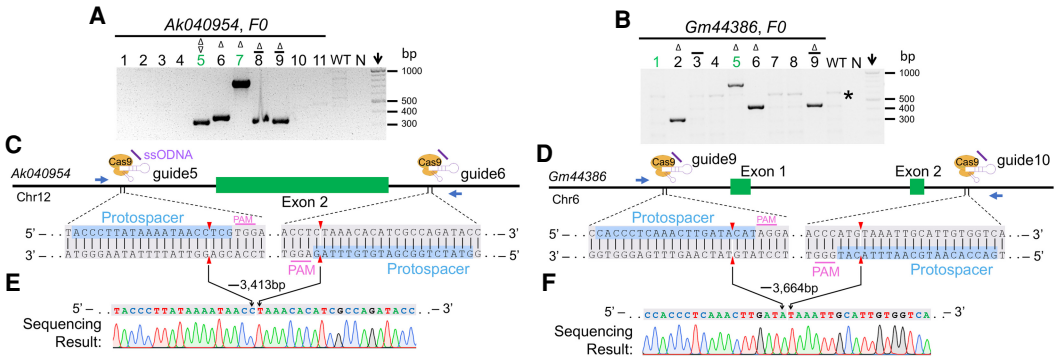

Figure 4. Null alleles of *Ak040954* and *Gm44386* genes generated by the *i*-GONAD method. (*A*,*B*) Genotyping results of *Ak040954* (*A*) and *Gm44386* (*B*) for the *F0* generation using primer pairs shown in C and *D*. The mice #5 to #9 in *A* and mice #2, #5, #6, and #9 in *B* showed large deletions. The star in *B* indicates a faint, nonspecific band. Note that WT or floxed alleles are too large to be detected in current PCR conditions. (*C*,*D*) Gene structures and positions of gRNA and genotyping primers for *Ak040954* (*C*) and *Gm44386* (*D*) genes. (*E*,*F*) Sanger sequencing results of founder #9 and #6 as shown in *A* and *B*, respectively. For all panels: (WT) wild-type, (N) negative control (water), green ID highlights founders with floxed alleles, (arrow) DNA marker lane, mice with single-side *loxP* integration are indicated by a bar over the ID, (Δ) deletions, (▽) large insertions.

Test of *i*-GONAD on the *Mecp2* gene

We continued to examine whether the short symmetric ssODNA donors can work for *i*-GONAD in generation of conditional alleles. For this purpose, we chose the *Mecp2* (methyl CpG binding protein 2) gene because multiple groups have attempted to insert *loxP* by microinjecting symmetric ssODNA donors (Yang et al. 2013; Gurumurthy et al. 2019a). As such, using the same designs of gRNA and ssODNA, it provides an indirect comparison of *i*-GONAD with the microinjection approach.

Three CD-1 female mice that showed copulation plugs after mating with C57BL/6J males were used for the *i*-GONAD procedure. Embryos at day 12.5 postconception (E12.5) were collected for genotyping analysis. The high efficiency of gRNAs was revealed by big truncations and possible elimination of primer binding sites in multiple samples (#1, #2, #4, #6, #9, #15) (Supplemental Fig. S9A,B). Among 19 total embryos, two showed a 5′-*loxP* site; four showed a 3′-*loxP* site, with one embryo (#3) showing both 5′- and 3′-*loxP* sites. Long-range PCR (Supplemental Fig. S9B) and cloning-based genotyping analysis (Supplemental Fig. S9C,D) confirmed in *cis loxP* insertions in this sample. These results were consistent with a previous report that the efficiency of *loxP* insertions in this locus was relatively low (Gurumurthy et al. 2019a).

Repeating *i*-GONAD on *Plagl1* and *Clcf1* genes using C57BL/6J females

i-GONAD can efficiently deliver CRISPR cocktails for a variety of hybrid or inbred mouse strains (Ohtsuka et al. 2018). We used CD-1 females because of their good postsurgery performance and generally large litter size. In our experience, performing *i*-GONAD on CD-1 females is also easier than C57BL/6J females thanks to larger volumes of the oviduct. However, with technical proficiency gained from these practices, we continued to determine whether conditional alleles could also be produced from the inbred C57BL/6J strain.

Plag1 and *Clcf1* genes were selected for these tests. C57BL/6J females that showed copulation plugs after mating with C57BL/6J males were used for *i*-GONAD. As previously observed, the pregnancy rate of C57BL/6J females was low (Ohtsuka et al. 2018). From multiple breeding pairs, only two females produced a total of five embryos for the *Plagl1* experiment, and another two females produced six for the *Clcf1* experiment. Nevertheless, we identified one embryo that showed a floxed allele for each gene (Fig. 5A,B), which was also confirmed by analyzing the long-range PCR products (Fig. 5C; Supplemental Fig. S10). Together, these results are in agreement with previous observations that inbred strains can be used for genome editing by the *i*-GONAD method (Ohtsuka et al. 2018).

Validation of the *Fosl1* conditional allele

We continued to validate the design and utility of the conditional allele that we generated by *i*-GONAD. Through serial crossing of *Fosl1*$^{loxP/loxP}$ with *Pax7*^{CreER} mice (Lepper et al. 2009), a widely used muscle stem cell–specific Cre deleter, we obtained *Pax7*^{CreER}:*Fosl1*$^{loxP/loxP}$ conditional knock out mouse model,

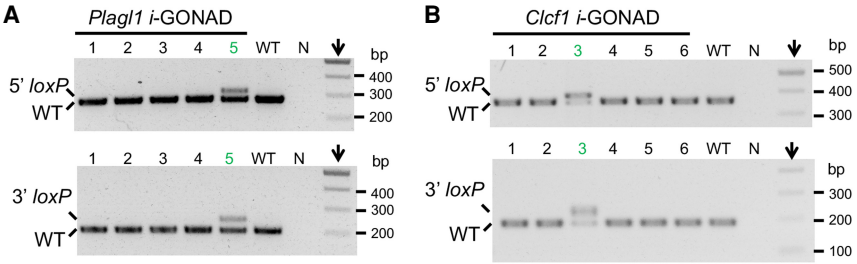

C

Gene Symbol	*F0* founder	*loxP* in cis	Single *loxP*		WT	Other	Total
			5′ *loxP*	3′ *loxP*			
Plagl1	#5	**7**	1	2	5	1	16
Clcf1	#3	**5**	0	0	10	1	16

Figure 5. Testing *i*-GONAD for generation of conditional alleles using C57BL/6J mice. (*A*) *Plagl1* genotyping results of E12.5 embryos. For the 5′ gRNA region, WT band is 278 bp, *loxP* band is 312 bp; for the 3′ gRNA region, WT band is 200 bp, *loxP* band is 234 bp. (*B*) *Clcf1* genotyping results for E12.5 embryos. For the 5′ gRNA region, WT band is 355 bp, *loxP* band is 389 bp; for the 3′ gRNA region, WT band is 188 bp, *loxP* band is 222 bp. (*C*) Summary of bacteria colony genotyping results shown in Supplemental Figure S10C,D.

indicated by *Fosl1*^{cKO}. Tamoxifen was administered into adult mutants to activate CreER and thus the removal of exons 3 and 4 of the *Fosl1* gene (Fig. 6A). Two days after the last dosage of tamoxifen, muscle tissues were collected for genotyping analyses. As expected, the recombined allele can be specifically detected in muscle samples from *Fosl1*^{cKO} but not littermate *Fosl1*$^{loxP/loxP}$ mice (Fig. 6B). Sequencing confirmed the correct recombination between 5′- and 3′-*loxP* sites that excised the targeted exons and joined intron 2 with the 3′ region of the *Fosl1* gene (Fig. 6C). Because muscle stem cells account for less than 5% of total nuclei in intact muscle tissues (Snow 1981), the intact floxed allele was also readily detected in *Fosl1*^{cKO} muscle samples (Fig. 6B).

We then isolated muscle precursor cells from *Fosl1*^{cKO} mouse and confirmed the robust inactivation of *Fosl1* gene detected by qPCR using primers from exon 4 of this gene (Fig. 6D). As a negative control, fibroblasts that were also isolated from *Fosl1*^{cKO} mouse showed a normal level of expression for the *Fosl1* gene (Fig. 6D). We did not examine *Fosl1* gene expression in whole muscle tissues because muscle precursor cells only account for a small portion of the tissue, whereas the remaining cell types (*Pax7*$^{-}$) also abundantly express the *Fosl1* gene, as shown by single-cell RNA sequencing analyses of muscle tissues (Supplemental Fig. S11; The Tabula Muris Consortium 2018). These results validated the utility of the conditional allele produced by the *i*-GONAD method.

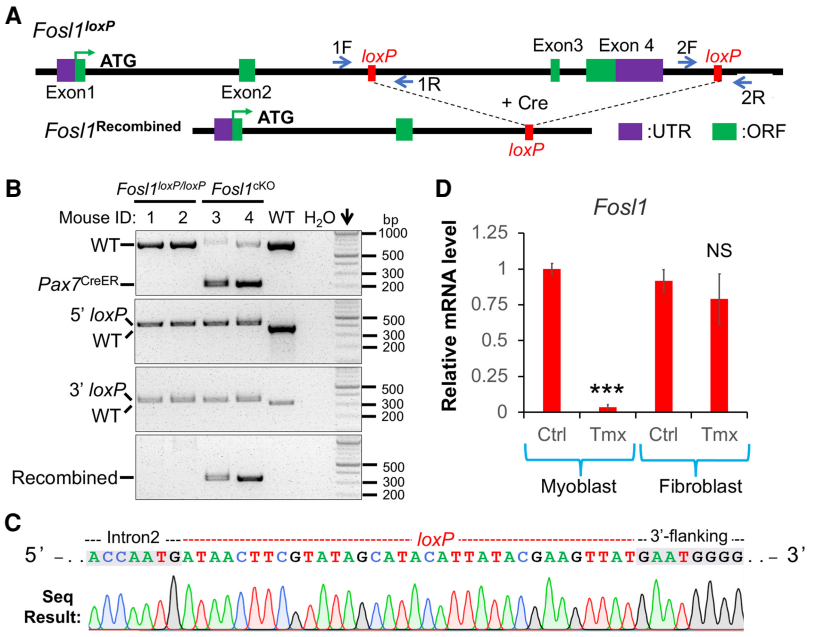

Figure 6. Successful recombination of the *Fosl1* floxed allele mediated by Cre. (*A*) Gene structures of the *Fosl1*^{loxP} and recombined alleles following Cre-mediated DNA recombination. (*B*) Genotyping results of adult muscle tissues from *Fosl1*$^{loxP/loxP}$ and littermate *Fosl1*^{cKO} mice. 5′- and 3′-*loxP* were detected by primers 1F + 1R and 2F + 2R, respectively. The floxed allele was detected by primers 1F + 2R. (*C*) Sanger sequencing result that validated DNA recombination in *Fosl1*^{cKO} muscle sample. (*D*) qPCR that measured *Fosl1* expression in myoblasts and fibroblasts isolated from the *Fosl1*^{cKO} mice. qPCR primers are located in exon 4 which is floxed. (Ctrl) Vehicle control, (Tmx) 4-OH tamoxifen. (***) $P < 0.001$, (NS) not significant. Data are mean ± SEM.

Discussion

The overall targeting efficiency of producing floxed alleles by *i*-GONAD was 10% (eight out of 76) (Table 1). In addition to these desired mutants, the frequency of obtaining *F0* mice with either 5′- or 3′-*loxP* insertion was 28% (21 out of 76). Therefore, the combined *loxP*-insertion efficiency was 38%, close to the HDR efficiency that was previously reported using the *i*-GONAD method (49%) or through microinjection (52%) (Ohtsuka et al. 2018). In *F1* generations, the chance of inheriting two *loxP* sites (in *cis*) was 37% (32 out of 87 pups) (Table 1), indicating efficient germline editing by *i*-GONAD. These tests demonstrate that our approach, using the *i*-GONAD method and the HDR template design, is robust, fast, and efficient for the generation of mouse conditional alleles.

One recent large-scale test of microinjection reported an 11% *loxP*-insertion efficiency by using asymmetric ssODNAs and a 7% efficiency by using symmetric ssODNAs (Lanza et al. 2018). Compared with these dual-ssODNA approaches, long ssODNA, composed of *loxP*–Exon(s)–*loxP* sequences, was shown to be more efficient in generating floxed alleles (Quadros et al. 2017; Lanza et al. 2018; Miura et al. 2018; Miyasaka et al. 2018). Because both *loxP* sites were synthesized in one piece, this predicts simultaneous integrations of two *loxP* sites. However, technical barriers do exist for the preparations of long ssODNA (Lanza et al. 2018). Depending on the length of the floxed area, production of long ssODNA that meets the required yield, purity, and fidelity by either chemical synthesis or enzymatic reactions is still challenging. For instance, even without considering the homology arms, the floxed regions for our genes measured 2–7 kb. In comparison, the maximum size of ssODNA (megamer) that can be ordered from IDT is 2 kb. Therefore, broader applications of long ssODNA await improvement of DNA synthesis technology.

In comparison with the conventional floxing method, an alternative strategy of conditional gene-inactivation by leveraging the exon-splicing machinery (Guzzardo et al. 2017) could make the use of single-piece ssODNA more realistic. This conditional knockout strategy involves the insertion of a small artificial intron that harbors two *loxP* sites into a coding exon of the target gene. In the absence of Cre, this foreign sequence can be fully excised by splicing machinery without affecting gene function. In the presence of Cre activity, recombination of *loxP* sites will destroy the artificial intron which causes translational termination, thus abrogating gene function. It remains to be tested whether the artificial-intron ssODNA can produce higher targeting efficiency when delivered by *i*-GONAD.

In addition to the formats of donors, the HDR efficiency can also be affected by donor concentration at the editing site (Liu et al. 2019). Consistent with this notion, HDR frequency was improved when ssODNA was chemically linked to Cas9 protein (Ma et al. 2017; Aird et al. 2018; Ling et al. 2020). In a simpler form, one can test whether the more stable ssODNA, improved by chemical modifications, can enhance *i*-GONAD efficiency. Other methods to improve HDR frequency include chemical inhibition of the nonhomologous end-joining pathway (Maruyama et al. 2015), engineering of Cas9 protein (Charpentier et al. 2018;

Table 1. Summary of *loxP* integration efficiency

	F0 generation				*F1* generation			
Gene	Only 5′ *loxP*	Only 3′ *loxP*	Two *loxPs*	# Genotyped	Only 5′ *loxP*	Only 3′ *loxP*	Two *loxPs*	# Genotyped
Fosl1	2	4	1	20	0	0	4	22
Plagl1	4	4	3	28	0	7	8	15
Ak040954	2	0	2	11	0	0	6	19
Clcf1	1	1	1	8	5	0	8	13
Gm44386	1	2	1	9	3	4	6	18
Totals	10 (13.2%)	11 (14.5%)	8 (10.5%)	76	8 (9.2%)	11 (12.6%)	32 (36.8%)	87

Jayavaradhan et al. 2019), and the timing of gene targeting in S/G2 phases of the cell-cycle (Lin et al. 2014). The *i*-GONAD procedure is performed around 4:00 p.m. of the day when the vaginal plug is observed (Ohtsuka et al. 2018; Gurumurthy et al. 2019b). This marks approximately 16 h post-insemination (hpi), a stage when zygotes transit from the S to the G2 phase of the first cell-cycle (Luthardt and Donahuc 1973; Howlett and Bolton 1985; Debey et al. 1989). In comparison, microinjection or ex vivo zygote electroporation was commonly performed at an earlier time that corresponds to 10–12 hpi (Lanza et al. 2018; Teixeira et al. 2018). The timing differences of these CRISPR delivery methods may affect the efficiency of *loxP* insertions.

One limitation of the current study is the relatively smaller number of genes tested, as compared with the larger-scale microinjection experiments (Lanza et al. 2018) or multicenter consortium studies (Gurumurthy et al. 2019a). Because we do not have access to microinjection core or ex vivo zygote electroporation setups, we cannot directly compare the performance of these delivery methods. However, the initial report of *i*-GONAD confirmed that its HDR efficiency was comparable with that achieved through microinjection (Ohtsuka et al. 2018). Similarly, the 10% efficiency that we observed for *loxP* insertions by *i*-GONAD was also comparable with that from microinjection (11%–12%) (Bi et al. 2018; Lanza et al. 2018), though locus-to-locus variability was observed. For instance, the efficiency of creating a floxed allele for the *Fosl1* gene is 5% (one out 20) versus 18% (two out 11) for the *Ak040954* gene (Table 1). This could be caused by different levels of chromatin accessibility, a major determinant of Cas9 binding and activity (Wu et al. 2014; Chari et al. 2015). Nevertheless, successful delivery of CRISPR reagents is required but certainly cannot guarantee the same editing efficiency for different loci.

To provide an indirect comparison with the microinjection method, we repeated *i*-GONAD on the *Mecp2* gene. We selected this locus because it was previously tested by the microinjection method, though a large discrepancy of targeting efficiency, ranging from 0% to 16%, was reported (Yang et al. 2013; Gurumurthy et al. 2019a). The *i*-GONAD efficiency of producing a floxed allele for this locus is 5%. Of note, the gRNAs did show high editing activity in producing null alleles. Therefore, *i*-GONAD is a reliable method to deliver the CRISPR cocktail into zygotes, and the efficiency of producing conditional alleles can vary largely at different loci.

We referred to our previous experience of microinjection (Bi et al. 2018) for the molar ratios of Cas9, gRNA, and ssODNA. It remains unknown whether other concentrations of these reagents could enhance the success rate of *i*-GONAD. Although *i*-GONAD does not require direct handling of the mouse embryo, its success depends on many factors. First, similar to microinjection, *i*-GONAD requires steady hand-control of the microcapillary needle for oviduct injection. Second, a thorough understanding of the mouse reproductive system is essential. In our experience, oviduct injections visualized by dye solution have afforded valuable training opportunities. In addition, we recommend testing gRNAs in cultured mouse cells, for example, fibroblasts, before applying them for *i*-GONAD. Last, one should monitor the off-target mutations in picked founders, especially when the predicted off-target site is located near the gene of interest. In summary, our study provides a complete gene targeting workflow to create, analyze, and authenticate conditional alleles. This may promote gene function studies in vivo by providing an inexpensive alternative to generate custom mouse models.

Methods

Oviduct electroporation by the *i*-GONAD protocol

All animal procedures were approved by the Institutional Animal Care and Use Committee (IACUC) at the University of Georgia. Mouse oviduct electroporation was performed as previously reported (Ohtsuka et al. 2018). Briefly, 6- to 10-wk-old CD-1 or C57BL/6J female mice were mated with C57BL/6J stud males the day before electroporation. The copulated female mice were used for surgery to expose the oviduct. CRISPR gene editing cocktails were freshly assembled and contained 6 μM Cas9 protein (IDT 1081058, Lot # 0000405530), 30 μM gRNA (Alt-R crRNA annealed with tracrRNA, IDT 1072534, Lot # 0000403961), and 18 μM ssODNA (IDT Ultramer DNA Oligo, standard desalting). This cocktail was delivered into the oviduct through microcapillary injection. Oviduct electroporation was performed using a CUY21EDIT II electroporator with the following protocol: Pd A: 100 mA, Pd on: 5 msec, Pd off: 50 msec, three cycles, decay 10%. The sequences for gRNA and ssODNA are provided in Supplemental Materials.

Mouse genotyping analysis

Genotyping PCR was performed using genomic DNA extracted from the toe clipping with the primers listed in Supplemental Materials. For Sanger sequencing, PCR products were first gel-purified and cloned into the pCRII Topo vector (Thermo Fisher Scientific K460001) and sequenced with T7 or SP6 primers. Long-range PCR was performed using LongAmp Hot Start Taq 2X Master Mix (NEB M0533S) to examine genomic DNA that was purified by a Monarch Genomic DNA Purification kit (NEB T3010). The large amplicons were gel-purified and cloned into the pCR-XL-2-TOPO vector (Thermo Fisher Scientific K8050-10). The top off-targeting sites were predicted by Cas-OFFinder (Bae et al. 2014).

Tamoxifen and muscle injury

Tamoxifen (Sigma-Aldrich T5648) was dissolved in ethanol (10 mg/mL). This stock solution was diluted in sesame oil (Sigma-Aldrich S3547) with a ratio of 1:9 before injection. Two

milligrams of tamoxifen were administered by intraperitoneal injection. Muscle injury was induced by injecting 1.2% barium chloride (50 μL) into the tibialis anterior muscle.

Competing interest statement

The authors declare no competing interests.

Acknowledgments

We thank Junfei Wen and Hector Romero-Soto for technical assistance. We also thank the Center for Molecular Medicine and the Complex Carbohydrate Research Center for administrative support and the IACUC and URAR team from the University of Georgia for mouse colony management. We thank Dr. Shihuan Kuang and Jun Wu from Purdue University and Dr. Xiaochun Li from the University of Texas Southwestern Medical Center for sharing reagents and Dr. Jonathan Eggenschwiler for critical reading of this manuscript. We also thank Dr. Masato Ohtsuka from Tokai University and Dr. Channabasavaiah Gurumurthy from the University of Nebraska Medical Center for consultations on the oviduct electroporation method and patient instructions and other members from the Bi lab for technical advice. This work was supported by start-up funding from the University of Georgia.

Author contributions: R.S., H.Z., and P.B. designed and performed the research; R.S. and P.B. analyzed the data; and P.B. wrote the paper.

References

Adli M. 2018. The CRISPR tool kit for genome editing and beyond. *Nat Commun* **9:** 1911. doi:10.1038/s41467-018-04252-2

Aida T, Chiyo K, Usami T, Ishikubo H, Imahashi R, Wada Y, Tanaka KF, Sakuma T, Yamamoto T, Tanaka K. 2015. Cloning-free CRISPR/Cas system facilitates functional cassette knock-in in mice. *Genome Biol* **16:** 87. doi:10.1186/s13059-015-0653-x

Aird EJ, Lovendahl KN, St Martin A, Harris RS, Gordon WR. 2018. Increasing Cas9-mediated homology-directed repair efficiency through covalent tethering of DNA repair template. *Commun Biol* **1:** 54. doi:10.1038/s42003-018-0054-2

Amoasii L, Long CZ, Li H, Mireault AA, Shelton JM, Sanchez-Ortiz E, McAnally JR, Bhattacharyya S, Schmidt F, Grimm D, et al. 2017. Single-cut genome editing restores dystrophin expression in a new mouse model of muscular dystrophy. *Sci Transl Med* **9:** eaan8081. doi:10.1126/scitranslmed.aan8081

Bae S, Park J, Kim JS. 2014. Cas-OFFinder: a fast and versatile algorithm that searches for potential off-target sites of Cas9 RNA-guided endonucleases. *Bioinformatics* **30:** 1473–1475. doi:10.1093/bioinformatics/btu048

Belteki G, Haigh J, Kabacs N, Haigh K, Sison K, Costantini F, Whitsett J, Quaggin SE, Nagy A. 2005. Conditional and inducible transgene expression in mice through the combinatorial use of Cre-mediated recombination and tetracycline induction. *Nucleic Acids Res* **33:** e51. doi:10.1093/nar/gni051

Bi P, McAnally JR, Shelton JM, Sánchez-Ortiz E, Bassel-Duby R, Olson EN. 2018. Fusogenic micropeptide Myomixer is essential for satellite cell fusion and muscle regeneration. *Proc Natl Acad Sci* **115:** 3864–3869. doi:10.1073/pnas.1800052115

Bouabe H, Okkenhaug K. 2013. Gene targeting in mice: a review. *Methods Mol Biol* **1064:** 315–336. doi:10.1007/978-1-62703-601-6_23

Capecchi MR. 1989. The new mouse genetics: altering the genome by gene targeting. *Trends Genet* **5:** 70–76. doi:10.1016/0168-9525(89)90029-2

Chari R, Mali P, Moosburner M, Church GM. 2015. Unraveling CRISPR-Cas9 genome engineering parameters via a library-on-library approach. *Nat Methods* **12:** 823–826. doi:10.1038/nmeth.3473

Charpentier M, Khedher AHY, Menoret S, Brion A, Lamribet K, Dardillac E, Boix C, Perrouault L, Tesson L, Geny S, et al. 2018. CtIP fusion to Cas9 enhances transgene integration by homology-dependent repair. *Nat Commun* **9:** 1133. doi:10.1038/s41467-018-03475-7

Chen J, Brunner AD, Cogan JZ, Nuñez JK, Fields AP, Adamson B, Itzhak DN, Li JY, Mann M, Leonetti MD, et al. 2020. Pervasive functional translation of noncanonical human open reading frames. *Science* **367:** 1140–1146. doi:10.1126/science.aay0262

Cheon DJ, Orsulic S. 2011. Mouse models of cancer. *Annu Rev Pathol-Mech* **6:** 95–119. doi:10.1146/annurev.pathol.3.121806.154244

Danielian PS, Muccino D, Rowitch DH, Michael SK, McMahon AP. 1998. Modification of gene activity in mouse embryos *in utero* by a tamoxifen-inducible form of Cre recombinase. *Curr Biol* **8:** 1323–1326. doi:10.1016/S0960-9822(07)00562-3

Debey P, Renard JP, Coppey-Moisan M, Monnot I, Geze M. 1989. Dynamics of chromatin changes in live one-cell mouse embryos: a continuous follow-up by fluorescence microscopy. *Exp Cell Res* **183:** 413–433. doi:10.1016/0014-4827(89)90401-1

Doudna JA, Charpentier E. 2014. Genome editing. The new frontier of genome engineering with CRISPR-Cas9. *Science* **346:** 1258096. doi:10.1126/science.1258096

Doyle A, McGarry MP, Lee NA, Lee JJ. 2012. The construction of transgenic and gene knockout/knockin mouse models of human disease. *Transgenic Res* **21:** 327–349. doi:10.1007/s11248-011-9537-3

Feil S, Valtcheva N, Feil R. 2009. Inducible Cre mice. *Methods Mol Biol* **530:** 343–363. doi:10.1007/978-1-59745-471-1_18

Fortin JP, Tan J, Gascoigne KE, Haverty PM, Forrest WF, Costa MR, Martin SE. 2019. Multiple-gene targeting and mismatch tolerance can confound analysis of genome-wide pooled CRISPR screens. *Genome Biol* **20:** 21. doi:10.1186/s13059-019-1621-7

Guo F, Gopaul DN, Van Duyne GD. 1997. Structure of Cre recombinase complexed with DNA in a site-specific recombination synapse. *Nature* **389:** 40–46. doi:10.1038/37925

Gurumurthy CB, Lloyd KCK. 2019. Generating mouse models for biomedical research: technological advances. *Dis Model Mech* **12:** dmm029462. doi:10.1242/dmm.029462

Gurumurthy CB, Takahashi G, Wada K, Miura H, Sato M, Ohtsuka M. 2016. GONAD: a novel CRISPR/Cas9 genome editing method that does not require ex vivo handling of embryos. *Curr Protoc Hum Genet* **88:** 15.18.1–15.18.12. doi:10.1002/0471142905.hg1508s88

Gurumurthy CB, O'Brien AR, Quadros RM, Adams J, Alcaide P, Ayabe S, Ballard J, Batra SK, Beauchamp MC, Becker KA, et al. 2019a. Reproducibility of CRISPR-Cas9 methods for generation of conditional mouse alleles: a multi-center evaluation. *Genome Biol* **20:** 171. doi:10.1186/s13059-019-1776-2

Gurumurthy CB, Sato M, Nakamura A, Inui M, Kawano N, Islam MA, Ogiwara S, Takabayashi S, Matsuyama M, Nakagawa S, et al. 2019b. Creation of CRISPR-based germline-genome-engineered mice without ex vivo handling of zygotes by i-GONAD. *Nat Protoc* **14:** 2452–2482. doi:10.1038/s41596-019-0187-x

Guzzardo PM, Rashkova C, Dos Santos RL, Tehrani R, Collin P, Bürckstümmer T. 2017. A small cassette enables conditional gene inactivation by CRISPR/Cas9. *Sci Rep* **7:** 16770. doi:10.1038/s41598-017-16931-z

Howlett SK, Bolton VN. 1985. Sequence and regulation of morphological and molecular events during the first cell cycle of mouse embryogenesis. *J Embryol Exp Morphol* **87:** 175–206.

Hsu PD, Lander ES, Zhang F. 2014. Development and applications of CRISPR-Cas9 for genome engineering. *Cell* **157:** 1262–1278. doi:10.1016/j.cell.2014.05.010

Irion U, Krauss J, Nusslein-Volhard C. 2014. Precise and efficient genome editing in zebrafish using the CRISPR/Cas9 system. *Development* **141:** 4827–4830. doi:10.1242/dev.115584

Jaisser F. 2000. Inducible gene expression and gene modification in transgenic mice. *J Am Soc Nephrol* **11**(Suppl. 16)**:** S95–S100.

Jayavaradhan R, Pillis DM, Goodman M, Zhang F, Zhang Y, Andreassen PR, Malik P. 2019. CRISPR-Cas9 fusion to dominant-negative 53BP1 enhances HDR and inhibits NHEJ specifically at Cas9 target sites. *Nat Commun* **10:** 2866. doi:10.1038/s41467-019-10735-7

Jiang FG, Doudna JA. 2017. CRISPR-Cas9 structures and mechanisms. *Annu Rev Biophys* **46:** 505–529. doi:10.1146/annurev-biophys-062215-010822

Jiang W, Marraffini LA. 2015. CRISPR-Cas: new tools for genetic manipulations from bacterial immunity systems. *Annu Rev Microbiol* **69:** 209–228. doi:10.1146/annurev-micro-091014-104441

Kaneko T, Mashimo T. 2015. Simple genome editing of rodent intact embryos by electroporation. *PLoS One* **10:** e0142755. doi:10.1371/journal.pone.0142755

Lanza DG, Gaspero A, Lorenzo I, Liao L, Zheng P, Wang Y, Deng Y, Cheng C, Zhang C, Seavitt JR, et al. 2018. Comparative analysis of single-stranded DNA donors to generate conditional null mouse alleles. *BMC Biol* **16:** 69. doi:10.1186/s12915-018-0529-0

Lepper C, Conway SJ, Fan CM. 2009. Adult satellite cells and embryonic muscle progenitors have distinct genetic requirements. *Nature* **460:** 627–631. doi:10.1038/nature08209

Lewandoski M. 2001. Conditional control of gene expression in the mouse. *Nat Rev Genet* **2:** 743–755. doi:10.1038/35093537

Limonta J, Pedraza A, Rodríguez A, Freyre FM, Barral AM, Castro FO, Lleonart R, Gracía CA, Gavilondo JV, de la Fuente J. 1995. Production of active anti-Cd6 mouse-human chimeric antibodies in the milk of

transgenic mice. *Immunotechnology* **1:** 107–113. doi:10.1016/1380-2933(95)00010-0
Lin S, Staahl BT, Alla RK, Doudna JA. 2014. Enhanced homology-directed human genome engineering by controlled timing of CRISPR/Cas9 delivery. *eLife* **3:** e04766. doi:10.7554/eLife.04766
Ling X, Xie B, Gao X, Chang L, Zheng W, Chen H, Huang Y, Tan L, Li M, Liu T. 2020. Improving the efficiency of precise genome editing with site-specific Cas9-oligonucleotide conjugates. *Sci Adv* **6:** eaaz0051. doi:10.1126/sciadv.aaz0051
Liu M, Rehman S, Tang X, Gu K, Fan Q, Chen D, Ma W. 2019. Methodologies for improving HDR efficiency. *Front Genet* **9:** 691. doi:10.3389/fgene.2018.00691
Luthardt FW, Donahuc RP. 1973. Pronuclear DNA synthesis in mouse eggs. An autoradiographic study. *Exp Cell Res* **82:** 143–151. doi:10.1016/0014-4827(73)90256-5
Ma M, Zhuang F, Hu X, Wang B, Wen XZ, Ji JF, Xi JJ. 2017. Efficient generation of mice carrying homozygous double-floxp alleles using the Cas9-Avidin/Biotin-donor DNA system. *Cell Res* **27:** 578–581. doi:10.1038/cr.2017.29
Mansour SL, Thomas KR, Capecchi MR. 1988. Disruption of the proto-oncogene *int-2* in mouse embryo-derived stem cells: a general strategy for targeting mutations to non-selectable genes. *Nature* **336:** 348–352. doi:10.1038/336348a0
Maruyama T, Dougan SK, Truttmann MC, Bilate AM, Ingram JR, Ploegh HL. 2015. Increasing the efficiency of precise genome editing with CRISPR-Cas9 by inhibition of nonhomologous end joining. *Nat Biotechnol* **33:** 538–542. doi:10.1038/nbt.3190
Matsuo K, Owens JM, Tonko M, Elliott C, Chambers TJ, Wagner EF. 2000. *Fosl1* is a transcriptional target of c-Fos during osteoclast differentiation. *Nat Genet* **24:** 184–187. doi:10.1038/72855
Miura H, Gurumurthy CB, Sato T, Sato M, Ohtsuka M. 2015. CRISPR/Cas9-based generation of knockdown mice by intronic insertion of artificial microRNA using longer single-stranded DNA. *Sci Rep* **5:** 12799. doi:10.1038/srep12799
Miura H, Quadros RM, Gurumurthy CB, Ohtsuka M. 2018. *Easi*-CRISPR for creating knock-in and conditional knockout mouse models using long ssDNA donors. *Nat Protoc* **13:** 195–215. doi:10.1038/nprot.2017.153
Miyasaka Y, Uno Y, Yoshimi K, Kunihiro Y, Yoshimura T, Tanaka T, Ishikubo H, Hiraoka Y, Takemoto N, Tanaka T, et al. 2018. CLICK: one-step generation of conditional knockout mice. *BMC Genomics* **19:** 318. doi:10.1186/s12864-018-4713-y
Modzelewski AJ, Chen S, Willis BJ, Lloyd KCK, Wood JA, He L. 2018. Efficient mouse genome engineering by CRISPR-EZ technology. *Nat Protoc* **13:** 1253–1274. doi:10.1038/nprot.2018.012
Ohtsuka M, Sato M, Miura H, Takabayashi S, Matsuyama M, Koyano T, Arifin N, Nakamura S, Wada K, Gurumurthy CB. 2018. *i*-GONAD: a robust method for *in situ* germline genome engineering using CRISPR nucleases. *Genome Biol* **19:** 25. doi:10.1186/s13059-018-1400-x
Platt RJ, Chen SD, Zhou Y, Yim MJ, Swiech L, Kempton HR, Dahlman JE, Parnas O, Eisenhaure TM, Jovanovic M, et al. 2014. CRISPR-Cas9 knockin mice for genome editing and cancer modeling. *Cell* **159:** 440–455. doi:10.1016/j.cell.2014.09.014
Qi LS, Larson MH, Gilbert LA, Doudna JA, Weissman JS, Arkin AP, Lim WA. 2013. Repurposing CRISPR as an RNA-guided platform for sequence-specific control of gene expression. *Cell* **152:** 1173–1183. doi:10.1016/j.cell.2013.02.022
Quadros RM, Miura H, Harms DW, Akatsuka H, Sato T, Aida T, Redder R, Richardson GP, Inagaki Y, Sakai D, et al. 2017. *Easi*-CRISPR: a robust method for one-step generation of mice carrying conditional and insertion alleles using long ssDNA donors and CRISPR ribonucleoproteins. *Genome Biol* **18:** 92. doi:10.1186/s13059-017-1220-4
Rasys AM, Park S, Ball RE, Alcala AJ, Lauderdale JD, Menke DB. 2019. CRISPR-Cas9 gene editing in lizards through microinjection of unfertilized oocytes. *Cell Rep* **28:** 2288–2292.e3. doi:10.1016/j.celrep.2019.07.089
Richardson CD, Ray GJ, DeWitt MA, Curie GL, Corn JE. 2016. Enhancing homology-directed genome editing by catalytically active and inactive CRISPR-Cas9 using asymmetric donor DNA. *Nat Biotechnol* **34:** 339–344. doi:10.1038/nbt.3481
Sato M, Miyagasako R, Takabayashi S, Ohtsuka M, Hatada I, Horii T. 2020. Sequential i-GONAD: an improved in vivo technique for CRISPR/Cas9-based genetic manipulations in mice. *Cells* **9:** 546. doi:10.3390/cells9030546
Sauer B, Henderson N. 1988. Site-specific DNA recombination in mammalian cells by the Cre recombinase of bacteriophage P1. *Proc Natl Acad Sci USA* **85:** 5166–5170. doi:10.1073/pnas.85.14.5166
Schonig K, Schwenk F, Rajewsky K, Bujard H. 2002. Stringent doxycycline dependent control of CRE recombinase *in vivo*. *Nucleic Acids Res* **30:** 134e. doi:10.1093/nar/gnf134
Schreiber M, Wang ZQ, Jochum W, Fetka I, Elliott C, Wagner EF. 2000. Placental vascularisation requires the AP-1 component Fra1. *Development* **127:** 4937–4948.
Skarnes WC. 2015. Is mouse embryonic stem cell technology obsolete? *Genome Biol* **16:** 109. doi:10.1186/s13059-015-0673-6
Skarnes WC, Rosen B, West AP, Koutsourakis M, Bushell W, Iyer V, Mujica AO, Thomas M, Harrow J, Cox T, et al. 2011. A conditional knockout resource for the genome-wide study of mouse gene function. *Nature* **474:** 337–342. doi:10.1038/nature10163
Snow MH. 1981. Satellite cell distribution within the soleus muscle of the adult mouse. *Anat Rec* **201:** 463–469. doi:10.1002/ar.1092010303
Square T, Romasek M, Jandzik D, Cattell MV, Klymkowsky M, Medeiros DM. 2015. CRISPR/Cas9-mediated mutagenesis in the sea lamprey *Petromyzon marinus*: a powerful tool for understanding ancestral gene functions in vertebrates. *Development* **142:** 4180–4187. doi:10.1242/dev.125609
Sternberg N, Hamilton D, Hoess R. 1981. Bacteriophage-P1 site-specific recombination. II. Recombination between *lox*P and the bacterial chromosome. *J Mol Biol* **150:** 487–507. doi:10.1016/0022-2836(81)90376-4
The Tabula Muris Consortium. 2018. Single-cell transcriptomics of 20 mouse organs creates a *Tabula Muris*. *Nature* **562:** 367–372. doi:10.1038/s41586-018-0590-4
Takahashi G, Gurumurthy CB, Wada K, Miura H, Sato M, Ohtsuka M. 2015. GONAD: Genome-editing via Oviductal Nucleic Acids Delivery system: A novel microinjection independent genome engineering method in mice. *Sci Rep* **5:** 11406. doi:10.1038/srep11406
Teixeira M, Py BF, Bosc C, Laubreton D, Moutin MJ, Marvel J, Flamant F, Markossian S. 2018. Electroporation of mice zygotes with dual guide RNA/Cas9 complexes for simple and efficient cloning-free genome editing. *Sci Rep* **8:** 474. doi:10.1038/s41598-017-18826-5
te Riele H, Maandag ER, Berns A. 1992. Highly efficient gene targeting in embryonic stem cells through homologous recombination with isogenic DNA constructs. *Proc Natl Acad Sci USA* **89:** 5128–5132. doi:10.1073/pnas.89.11.5128
Thomas KR, Capecchi MR. 1987. Site-directed mutagenesis by gene targeting in mouse embryo-derived stem-cells. *Cell* **51:** 503–512. doi:10.1016/0092-8674(87)90646-5
Wang HY, Yang H, Shivalila CS, Dawlaty MM, Cheng AW, Zhang F, Jaenisch R. 2013. One-step generation of mice carrying mutations in multiple genes by CRISPR/Cas-mediated genome engineering. *Cell* **153:** 910–918. doi:10.1016/j.cell.2013.04.025
Wang HF, La Russa M, Qi LS. 2016a. CRISPR/cas9 in genome editing and beyond. *Annu Rev Biochem* **85:** 227–264. doi:10.1146/annurev-biochem-060815-014607
Wang W, Kutny PM, Byers SL, Longstaff CJ, DaCosta MJ, Pang C, Zhang Y, Taft RA, Buaas FW, Wang H. 2016b. Delivery of Cas9 protein into mouse zygotes through a series of electroporation dramatically increases the efficiency of model creation. *J Genet Genomics* **43:** 319–327. doi:10.1016/j.jgg.2016.02.004
Wu X, Scott DA, Kriz AJ, Chiu AC, Hsu PD, Dadon DB, Cheng AW, Trevino AE, Konermann S, Chen S, et al. 2014. Genome-wide binding of the CRISPR endonuclease Cas9 in mammalian cells. *Nat Biotechnol* **32:** 670–676. doi:10.1038/nbt.2889
Yang H, Wang HY, Shivalila CS, Cheng AW, Shi LY, Jaenisch R. 2013. One-step generation of mice carrying reporter and conditional alleles by CRISPR/Cas-mediated genome engineering. *Cell* **154:** 1370–1379. doi:10.1016/j.cell.2013.08.022
Yoshimi K, Kunihiro Y, Kaneko T, Nagahora H, Voigt B, Mashimo T. 2016. ssODN-mediated knock-in with CRISPR-Cas for large genomic regions in zygotes. *Nat Commun* **7:** 10431. doi:10.1038/ncomms10431
Yuan TT, Zhong Y, Wang YG, Zhang T, Lu R, Zhou MY, Lu YY, Yan KN, Chen YJ, Hu ZH, et al. 2019. Generation of hyperlipidemic rabbit models using multiple sgRNAs targeted CRISPR/Cas9 gene editing system. *Lipids Health Dis* **18:** 69. doi:10.1186/s12944-019-1013-8
Zhang JP, Li XL, Li GH, Chen WQ, Arakaki C, Botimer GD, Baylink D, Zhang L, Wen W, Fu YW, et al. 2017. Efficient precise knockin with a double cut HDR donor after CRISPR/Cas9-mediated double-stranded DNA cleavage. *Genome Biol* **18:** 35. doi:10.1186/s13059-017-1164-8
Zhu X, Xu Y, Yu S, Lu L, Ding M, Cheng J, Song G, Gao X, Yao L, Fan D, et al. 2014. An efficient genotyping method for genome-modified animals and human cells generated with CRISPR/Cas9 system. *Sci Rep* **4:** 6420. doi:10.1038/srep06420
Zijlstra M, Li E, Sajjadi F, Subramani S, Jaenisch R. 1989. Germ-line transmission of a disrupted β_2-microglobulin gene produced by homologous recombination in embryonic stem cells. *Nature* **342:** 435–438. doi:10.1038/342435a0
Zu Y, Zhang XS, Ren JF, Dong XH, Zhu Z, Jia L, Zhang QH, Li WM. 2016. Biallelic editing of a lamprey genome using the CRISPR/Cas9 system. *Sci Rep-Uk* **6:** 23496. doi:10.1038/srep23496

Received May 1, 2020; accepted in revised form November 16, 2020.